Multiaxial Variable Amplitude Loading for Automotive Parts Fatigue Life Assessment: A Loading Classification-based Approach Proposal

Enora Bellec, Matteo Facchinetti, Cédric Doudard, S. Calloch, Sylvain Moyne

Available online at www.sciencedirect.com

ScienceDirect

Structural Integrity Procedia 00 (2021) 000–000

Structural Integrity Procedia

www.elsevier.com/locate/procedia

FATIGUE DESIGN 2021, 9th Edition of the International Conference on Fatigue Design

Multiaxial Variable Amplitude Loading for Automotive Parts Fatigue Life Assessment: A Loading Classification-based Approach Proposal

E. Bellec[a,b], M.L. Facchinetti[a], C. Doudard[b], S. Calloch[b], S. Moyne[b]*

[a]*Stellantis (ex Groupe PSA), Chassis System Engineering, Voujeaucourt 25420, France*
[b]*ENSTA Bretagne, IRDL- UMR CNRS 6027, Brest 29200, France*

Abstract

This work reports the different steps of a frequency decomposition method applied for fatigue lifetime assessment. The studied loadings are multiaxial time series measured at the vehicle wheel. The proposed decomposition presupposes that the loading results from both dynamic vehicle effects at low frequencies (Driven Road loadings) and random loads at high frequencies (Random Road loadings). This signal partition has two assets for fatigue purposes. First, the spectral methods can be applied to the Random effects. Two spectral damage formulations are tested in this paper. Then, the Driven Road loadings, related to the vehicle manoeuvre, enables to implement the Rainflow counting method on only one time series instead of the initial set of six per wheel, or twelve per axle. The implemented approach illustrated on a braking manoeuvre is validated, comparing the damage summation of the Random and Driven Road loadings with the one based on the usual Rainflow counting method applied to the overall time series.

Keywords: life assessment ; multiaxial variable amplitude loading ; automotive chassis system

* Corresponding author.
E-mail address: enora.bellec@ensta-bretagne.org

1. Introduction

This study focuses on multiaxial life assessment method based on Variable Amplitude Loading (VAL) applied in the automotive industry, notably for the chassis system. In the scope of high cycle fatigue, all loadings are supposed to happen below the structure yield threshold. The data of interest introduced in this paper are loading time series (forces and torques) measured at the wheels, while the vehicle performs specific manoeuvres on the manufacturer proving ground (Grubisic (1994)).

For fatigue purposes, the measured forces and torques to consider usually gather six time series per wheel, thus twelve per axle (Sonsino et al. (2015)). Taking into account the overall data available from the wheels up to all different points of interest of the chassis system represents too much data to process. The usual cycle counting method applied for uniaxial life assessment purpose is the Rainflow counting one (Matsuishi and Endo (1968), Richlik (1987)). This method is accurate, easy to process at the wheel measurements, but loses the time information per cycle, thus the time correlation between different wheel measurements for multiaxial case. While studying the signals at the wheels two types of loadings stand out (Decker (2020)), as they differ regarding the load source and also the time-correlation nature between the measured channels:

- The Driven Road loadings: manoeuvres such as cornering and braking
- The Random Road loadings: vibratory and random loads coming from the road surface asperity

The goal of this work is to set a relevant loading decomposition method to develop a multiaxial life assessment method for chassis system components from the loading measured at the wheels. The first part of the paper depicts the theoretical local stress formulation inside the chassis part based on the above loading partition. It details the overall implemented approach to cope with both signal sets. Then, the loading type partition is illustrated, using braking manoeuvre time series. Finally, the life assessment method is performed on the same example, using spectral methods to deal with Random Road loadings and usual Rainflow Counting method for the Driven Road ones.

Nomenclature

S	Loading amplitude vector
S_i	Loading amplitude numbered i
N_i	Number of cycles to failure corresponding to the constant amplitude S_i
n_i	Number of cycles performed at a given amplitude range S_i
b	Basquin equation exponent
C	Basquin parameter
D	Damage value
d_i	Damage induced at a given amplitude range S_i
D_R, D_D	Damage induced respectively by the Random Road and the Driven Road loadings
D_{RFC}	Damage calculated using the Rainflow counting method
$E_R[D]$	Damage expectancy value applying the Rayleigh's approximation
$E_{SM}[D]$	Damage expectancy value applying the Single Moment's approximation
$\underline{\underline{\sigma^{loc}}}$	Local stress tensor at the structure point of interest
$\underline{\underline{\sigma}}^{loc,L_i}\|_{L_i=1}$	Local stress tensor for a unitary level of Loading L_i
$E_{SM}[D]$	Damage expectancy value applying the Single Moment's approximation
ϕ	Power spectral density
m_i	Spectral moment, ordered i
ν_p	Peak occurrence frequency
ν_0^+	Zero-crossing rate
$p_p(S)$	Peaks probability density functions
$F_X, F_Y, F_Z, M_X, M_Y, M_Z$	Three forces and three torques measured per wheel

L_i	Loading numbered i, $i \in [\![1,12]\!]$
L_i^{DR}	Driven Road Loading numbered i
L_i^{RR}	Random Road Loading numbered i
S_m^{DR}	Master signal defined among the Driven Road loadings
$\alpha_{L_i S_m}^{DR}$	"Driven" coefficient between the signal L_i and the Master signal
$\alpha_{L_i L_1}^{SO}$	Orientation coefficient between the tensor related to L_i and the one related to L_1
$\boldsymbol{Q}$	Orientation coefficient matrix
M	Vehicle mass
R	Radius of the wheel
h	Vehicle center of gravity height
e	Vehicle wheelbase
η	Braking force rate applied on one wheel

2. Local stress formulation within the chassis system

2.1. Assumptions on loading type

As mentioned above, two types of loadings are extracted from the initial time series measurement: the Driven Road (DR) loadings and the Random Road (RR) ones. The partition between both effects is achieved using a basic low-pass filter, allowing to extract the DR loadings. The Fig. 1 illustrates the initial single time series measurement compared to its related DR b) and RR c) signals once the overall partition process is completed.

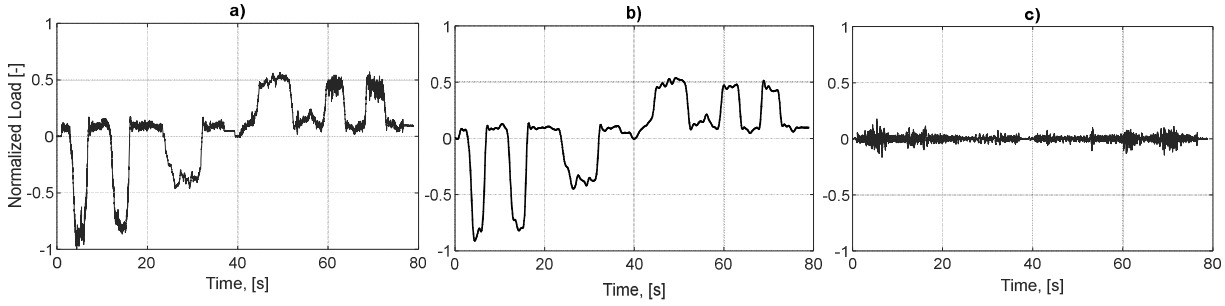

Fig. 1: (a) initial F_y load measurement on one wheel (b) DR loadings (c) RR loadings while performing a series of cornering

This partition process is performed for each time series included in the usual 6 DOF per wheel recordings, respectively. The initial measure $L_i(t)$ is equal to the sum of the DR and the RR loadings.

$$L_i(t) = L_i^{DR}(t) + L_i^{RR}(t). \quad (1)$$

Reasonably, for a same studied manoeuvre, every DR loadings extracted are time-correlated to each other. In other words, a correlation coefficient exists between two DR loadings.

Appointing a Driven "Master Signal", noted S_m^{DR}, eases the life assessment overall process. This enables to achieve the Rainflow counting on only one time signal (instead of performing Rainflow counting on the complete set of 6 DOF per wheel or 12 DOF per axle signals). Once the loading spectrum is determined on S_m^{DR}, i.e. number of cycles per amplitude class, multiplying the amplitude classes per the corresponding $\alpha_{L_i S_m}^{DR}$ coefficient gives the loading spectrum corresponding to the L_i^{DR} loading.

2.2. Structure influence on the stress tensor

Usually, the fatigue life assessment method is based on the variation of the stress tensor at the component's point of interest. As this paper mainly deals with the global loading (i.e. the input load at the vehicle wheels), it would be relevant to validate the signal partition process before tackling the different stress tensor configurations inside any chassis' part. To do so, some hypothesis about the stress tensor are made so that the time history $L_i(t)$ may directly appears in the stress tensor formula. Besides, anticipating the stress tensor shape may highlight what loading information is of interest regarding the ones measured at the wheel for the overall fatigue design method. For automotive design, the stress tensor on each axle depends upon the twelve loadings perceived at the axle's wheels. To build up the method, the linearity hypothesis is determined toward the relationship between the stress tensor and the measured time series such as

$$\underline{\underline{\sigma^{loc}(t)}} = \sum_i \underline{\underline{\sigma}}^{loc,\,L_i}|_{L_i=1} * L_i(t). \tag{2}$$

Taking into account the signal partition presented before, the stress tensor formulation turns out to be

$$\underline{\underline{\sigma^{loc}(t)}} = S_m^{DR}(t) * \left[\sum_i \underline{\underline{\sigma}}^{loc,\,L_i}|_{L_i=1} * \alpha_{L_i S_m}^{DR}\right] + \sum_i \underline{\underline{\sigma}}^{loc,\,L_i}|_{L_i=1} * L_i^{RR}(t). \tag{3}$$

The random part of this formula represents a sum of time-depending matrices. To lift this difficulty and check the validity of the proposed loading partition directly on the signal measured at the wheel, another assumption is made about the stress tensor shape: the stress tensor orientation is determined only by the structure itself no matter the loading axis. This assumption is notably respected at some critical points at the vicinity of welded joints. Thus, one can define a coefficient, noted $\alpha_{L_i L_j}^{SO}$, between two unitary loadings tensor such as

$$\underline{\underline{\sigma}}^{loc,\,L_i}|_{L_i=1} = \alpha_{L_i L_j}^{SO} * \underline{\underline{\sigma}}^{loc,\;\;L_j}|_{L_j=1}. \tag{4}$$

Combining both hypothesis Linearity *(2)* and Stress tensor orientation *(4),* the stress tensor at the point of interest reads

$$\underline{\underline{\sigma^{loc}(t)}} = \underline{\underline{\sigma}}^{loc,\;\;L_1}|_{L_1=1} * \left\{S_m^{DR}(t) * \left[\sum_i \alpha_{L_i L_1}^{SO} * \alpha_{L_i S_m}^{DR}\right] + \sum_i \alpha_{L_i L_1}^{SO} * L_i^{RR}(t)\right\}. \tag{5}$$

The stress tensor equation part depending on the time series represents an equivalent time signal. To ease the fatigue method validation at this point, the implemented approach within this paper does not consider the tensor shape induced by $\underline{\underline{\sigma}}^{loc,\;\;L_1}|_{L_1=1}$.

2.3. Implemented approach

To validate the implemented approach applied to the time series, the damage induced by the equivalent time signal is studied. As this paper does not focus on any particular part of the chassis system, no special material properties are used to define the damage model. To validate the initial "treatment" partition process applied to the wheel signals, a damage index is calculated based on the Basquin equation, (Basquin, (1919)) and the Palmgren-Miner summation rule (Palmgren, (1924), Miner, (1945)). Arbitrarily, the coefficients of the Basquin equation are fixed to b=4 and C=1, respectively

$$D = \sum_i d_i = \sum_i \frac{n_i}{N_i} = \sum_i \frac{n_i S_i^b}{C}. \tag{6}$$

The damage calculation differs depending on the loading type considered. For the DR loadings, the master signal corresponding to the manoeuvre and its associated coefficient $\alpha_{L_i S_m}^{DR}$ should be defined. Then the Rainflow counting method is only applied on $S_m^{DR}(t)$. The resulting loading spectrum is used to calculate the "Driven" damage index linked to the $S_m^{DR}(t) * \left[\sum_i \alpha_{L_i L_1}^{SO} * \alpha_{L_i S_m}^{\mathrm{DR}}\right]$ part. Regarding the RR loadings, $\sum_i \alpha_{L_i L_1}^{SO} * L_i^{RR}(t)$, the use of spectral methods enables to consider only the frequency-linked data and not the overall time-series to assess the fatigue life (Preumont, (1994)). These methods leads to a damage expectancy and not a fixed value. As depicted in the Fig. 2, the damage index is the expectancy considering both effects.

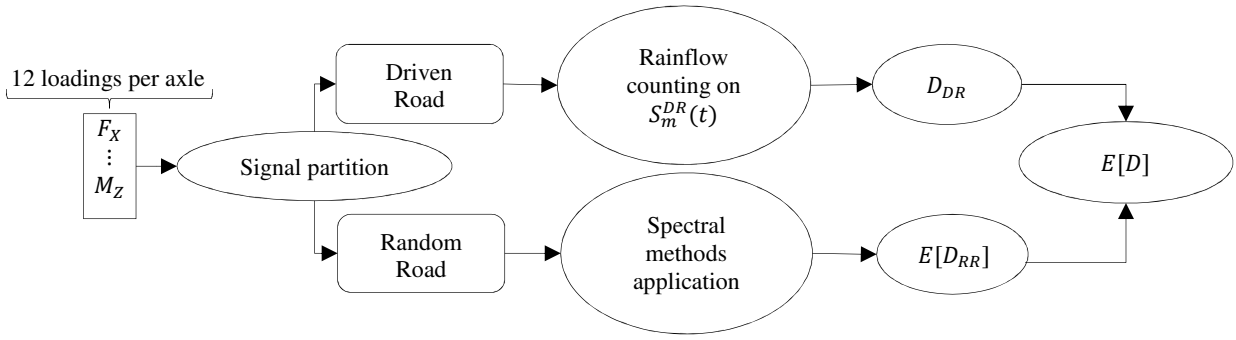

Fig. 2 : Signal partition and life assessment method methodology

3. Loading partition, during a braking manoeuvre

3.1. Vehicle dynamics

This paper applies the proposed method focusing on the braking manoeuvre study case. Before dealing with the measured time series, the correlated signals (i.e. DR loadings) are defined based on the expected vehicle dynamics. The braking manoeuvre is an overall movement along the car longitudinal axis. If considered along a straight line, we expect symmetric loads on left & right wheels. The Table 1 depicts the six loadings measured on each wheel, showing which ones are relevant during the braking manoeuvre and the theoretical relationships linking them to the longitudinal acceleration γ_x.

Table 1. Loadings related to the braking manoeuvre and following dynamics equations, on one wheel

Loading related to the manoeuvre	Loading Formula	Loading not related to the manoeuvre
F_X	$\frac{M\gamma_x}{\eta}$	F_Y
F_Z	$\frac{M\gamma_x h}{2e}$	M_X
M_Y	$-\frac{M\gamma_x}{\eta}R$	M_Z

At each wheel, only F_X, F_Z and M_Y are affected by the manoeuvre, through some basic vehicle length scales such as h, e, R, and the brake rate setup, η (cf. nomenclature table). The master signal S_m^{DR}, presented above, is determined to be the vehicle longitudinal acceleration γ_x.

3.2. Driven Road and Random Road loadings partition

Based on the theoretical definition, the braking manoeuvre master signal S_m^{DR} extracted from γ_x time-series is depicted in Fig. 3.

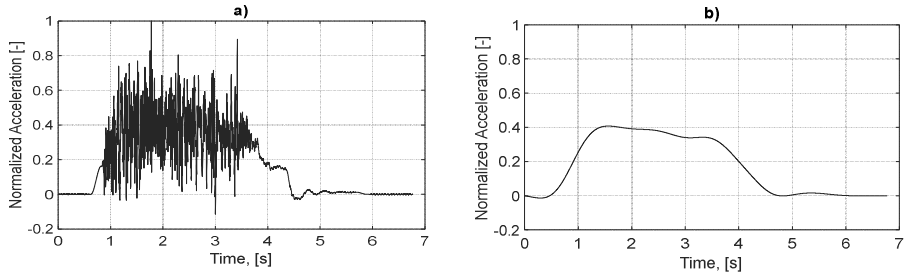

Fig. 3 : (a) initial γ_X acceleration measurement, (b) γ_X master signal definition

The master signal being defined, the overall partition process can be applied to each of the time series measured at the wheel. The Fig. 4 depicts this process for each of the six loading axis.

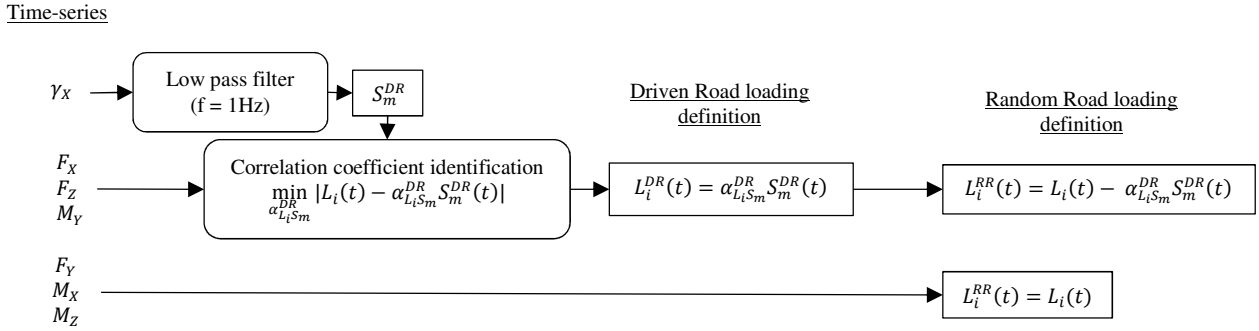

Fig. 4 : Driven and Random Road loadings definition from the time-series, braking manoeuvre case

Once the theoretical framework is determined, we now focus in detail on the loading time series actually measured at the wheels. The Fig. 5 a) highlights the initial measured F_X signal at one wheel on the front axle. The Fig. 5 is completed by the graphs b) and c) representing respectively the corresponding DR loading and the RR one. The same results as the one seen on the F_X signal are also visible when studying the F_Z and M_Y signals.

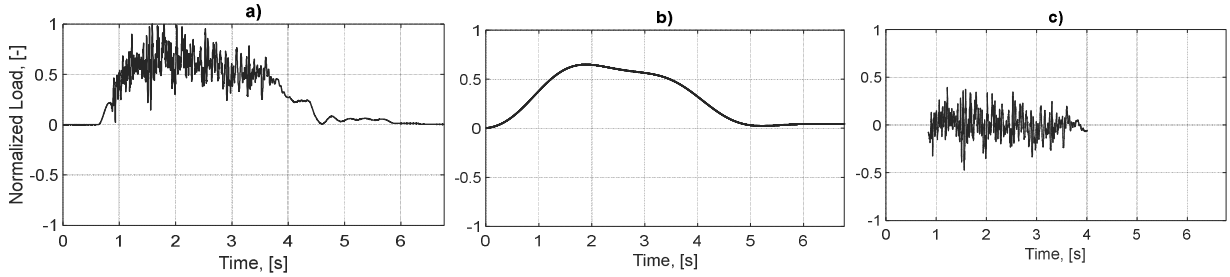

Fig. 5 : Braking load case: (a) initial F_X loading measurement on one-wheel (b) F_X DR loading (c) F_X RR loading

Comparing the F_X load shape to the F_Y one, it is clear that the manoeuvre (see S_m^{DR} on Fig. 3 b)) has no relevant impact on the F_Y signal. The Fig. 6 highlights the measured F_Y signal at the same wheel and the resulting RR loading. The same results as the one seen on the F_Y signal are also visible when studying the M_X and M_z signals.

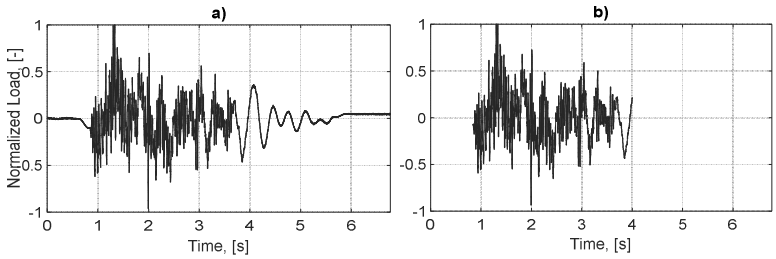

Fig. 6 : (a) initial F_Y loading measurement on one-wheel (b) F_Y RR loading while performing a braking

Now that the partition method, depicted in Fig. 4, is applied to all the time-series, the RR ones are further processed. Indeed, the final RR signals studied are only corresponding to the braking manoeuvre. Please note that the very first and last seconds of measurement do not transcribe the same random-like measurements (nearly vanishing variations). Thus, it is of no use for this study and they are cut off.

4. Lifetime assessment method application, during a braking manoeuvre

4.1. Spectral methods implementation

In the literature there are several methods dealing with fatigue life assessment based on random loadings (Pitoiset (2001), Rognon (2013), Mršnik et al (2013)). These methods are already at use to deal with vibratory loading by some car manufacturer (Decker (2020)). They are relevant for such loadings type, as they do not need to consider the loading time series information but only the signal frequency features. Hence, as the loading is acknowledged random, a multiplicity of time-series may correspond to the same loading frequency-based feature. To apply these methods, the studied random process should meet some requirements. As the overall process is considered stationary, the studied sample should be ergodic. Its distribution should be Gaussian and its average value equal to zero. The Fig. 7 highlights the signal distribution of the initial F_X measurement a) and the corresponding Random one b), both compared to a Gaussian distribution.

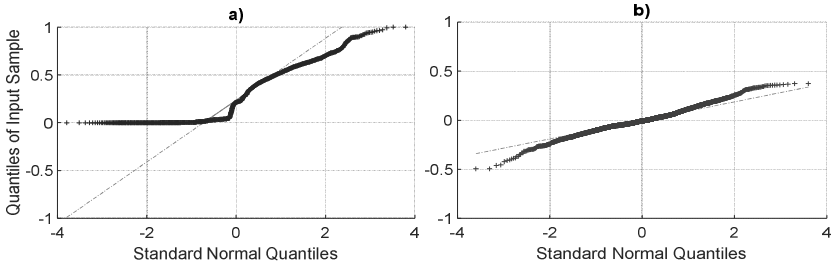

Fig. 7 : Gaussian distribution comparison: (a) initial F_X loading (b) RR F_X loading

The initial signal partition is imperative to apply the spectral methods. The Fig. 7 highlights how the partition eases these methods application, as the initial measurements do not meet the above basic hypothesis. The power spectral density linked to the RR loading is calculated. This frequency-based quantity contains the signal power per frequency interval. It is calculated from the Fourier transform of the signal autocorrelation function, $\phi_{L_i^{RR}L_i^{RR}}(f)$.

The power spectral density is the initial value used to calculate the spectral moments m_i. For a stationary zero-mean Gaussian process, Rice (Rice (1945)) developed the expected positive zero-crossing rate ν_0^+ and the peak occurrence frequency ν_p: both values are based on the spectral moments. Knowing these two rates, ν_0^+ and ν_p, it is then possible to estimate the number of loading cycles applied for a given period. The only missing information is the loading amplitudes of these cycles. Cartwright and Longuet-Higgins (Cartwright and Longuet-Higgins (1956)) define the peaks probability density functions $p_p(S)$ as a sum of a Rayleigh's and a Gaussian distribution. The contribution of damage ratio $\Delta(S)dS$ per cycle ($n_i = 1$) is formulated from the peak distribution, the peak frequency

and the damage per amplitude range, giving

$$\Delta(S)ds = \frac{S_i^b}{C} \nu_p p_p(S) dS. \tag{7}$$

Hence, the damage ratio integration on the amplitude scale results in the overall damage per unit time. Miles, (Miles (1954)) defines the damage expectancy per unit time for narrow band signal, named Rayleigh approximation

$$E_R[D] = \int_0^{+\infty} \Delta(S)dS = C^{-1} \frac{2^{\frac{b}{2}}}{2\pi} \Gamma\left(1+\frac{b}{2}\right) m_0^{\frac{b-1}{2}} m_2^{\frac{1}{2}}. \tag{8}$$

Numerous approximations inspired from this result exist in the literature, (Benasciutti and Tovo (2004)). Some of them change the Gaussian distribution by a Weibull distribution in the peak's probability density functions. The Rayleigh approximation fits for the narrow-band signal. Another approximation developed by Larsen and Lutes (Larsen and Lutes (1990)) is an empiric one, designed for wider band signal, using only one spectral moment. That is why it is named the Single Moment (SM) approximation, that reads

$$E_{SM}[D] = \int_0^{+\infty} \Delta(S)dS = C^{-1} \frac{2^{\frac{b}{2}}}{2\pi} \Gamma\left(1+\frac{b}{2}\right) m_2^{\frac{b}{2}}. \tag{9}$$

These two damage expectancies are applied to illustrate the use of spectral life assessment methods on the RR loading. The resulting values are compared to a reference one defined using the usual Rainflow counting method on the same time series. The proving signal is the sum of all the RR loadings (all the coefficient $\alpha_{L_i L_1}^{SO}$ are fixed to 1) measured on the front axle while performing the braking manoeuvre. The Fig. 8 illustrates the resulting RR loading.

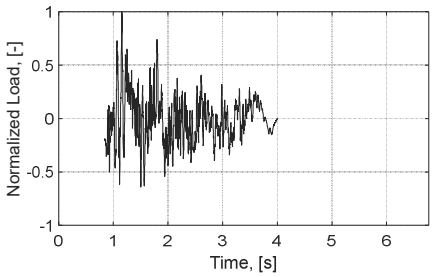

Fig. 8 : Equivalent Random Road loading, $\sum_i \alpha_{L_i L_1}^{SO} * L_i^{RR}(t)$

The Rainflow counting method is applied to this time series. Then the damage, based on the introduced Basquin equation, is calculated and compared to both of the damage expectancy values resulting from the use of spectral methods. For multiaxial case, Pitoiset, (Pitoiset (2001)), depicts a method based on the power spectral density matrix $\boldsymbol{\phi(f)}$, and orientation coefficient matrix, $\boldsymbol{Q}$. (When dealing with two different signals the power spectral density $\phi_{L_i^{RR} L_j^{RR}}(f)$. is based on the intercorrelation function). This approach leads to an equivalent power spectral density, $\phi_{eq}(f)$, on which perform the damage expectancy calculation

$$\phi_{eq}(f) = trace\big(\boldsymbol{Q} * \boldsymbol{\phi(f)}\big), \tag{10}$$

with

$$\boldsymbol{Q} = \begin{pmatrix} {\alpha_{L_1 L_1}^{SO}}^2 & \cdots & \alpha_{L_1 L_{12}}^{SO} \alpha_{L_{12} L_1}^{SO} \\ \vdots & \ddots & \vdots \\ \alpha_{L_1 L_{12}}^{SO} \alpha_{L_{12} L_1}^{SO} & \cdots & {\alpha_{L_{12} L_{12}}^{SO}}^2 \end{pmatrix} \text{and } \boldsymbol{\phi(f)} = \begin{pmatrix} \phi_{L_1^{RR} L_1^{RR}}(f) & \cdots & \phi_{L_1^{RR} L_{12}^{RR}}(f) \\ \vdots & \ddots & \vdots \\ \phi_{L_{12}^{RR} L_1^{RR}}(f) & \cdots & \phi_{L_{12}^{RR} L_{12}^{RR}}(f) \end{pmatrix} \tag{11}$$

The Table 2 highlights the different results from the damage calculations.

Table 2. Damage comparison with spectral methods, Random Road loading, Braking manoeuvre

D_R *or* $E[D_R]$	Value [-]	Gap % with $D_{R_{RFC}}$
$D_{R_{RFC}}$	$8{,}03E+11$	-
$E_R[D_R]$	$8{,}21E+11$	2 %
$E_{SM}[D_R]$	$3{,}23E+11$	60 %

As the Basquin law coefficients are fixed to arbitrary parameters ($b = 4, C = 1$), the resulting damage amounts are simply damage indices. Compared to the reference value, the spectral methods result gives the same order of magnitude, especially the Rayleigh formula, for this study case.

4.2. Method validation

To validate the overall signal partition method, a proving set of time series is made of the twelve initial time-series on a vehicle axle (here again the coefficient $\alpha_{L_iL_1}^{SO}$ are fixed to 1). The Fig. 9 represents the resulting signal on which is performed the reference method (i.e. Rainflow counting method and damage calculation).

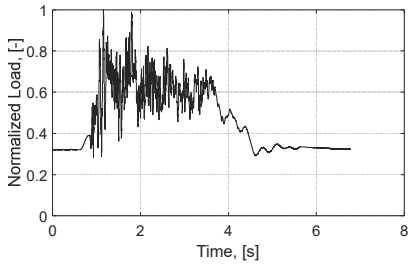

Fig. 9 : Equivalent overall time measured loading, $S_m^{DR}(t) * \left[\sum_i \alpha_{L_iL_1}^{SO} * \alpha_{L_iS_m}^{DR}\right] + \sum_i \alpha_{L_iL_1}^{SO} * L_i^{RR}(t)$

In Table 3 the damage reference value is compared to the sum of the damage induced by the RR loadings and the DR ones. The "Driven" coefficients are defined for each of the three axis involved per wheel, following the method depicted in Fig. 4. As expected these values are close to the ones expected in Table 1. The Rainflow counting method is once again performed only on the master signal γ_x. The corresponding DR loadings spectra are all ensue from it. Then, the overall $D_{D_{RFC}}$ $(1.94e+10)$ damage results as the sum of the different damage calculated per axis following the $\alpha_{L_iL_1}^{SO}$ unit value. The sum between $D_{D_{RFC}}$ and the damage expectancy based on the RR loading leads to an overall damage expectancy. The Table 3 highlights these results.

Table 3. Damage comparison resulting from the overall partition method, RR and DR loadings, Braking manoeuvre

D *or* $E[D]$	Value [-]	Gap % with $D_{R_{RFC}}$
D_{RFC}	$8.77E+11$	-
$D_{R_{RFC}} + D_{D_{RFC}}$	$8{,}22E+11$	6 %
$E_R[D_R] + D_{D_{RFC}}$	$8{,}40E+11$	4 %
$E_{SM}[D_R] + D_{D_{RFC}}$	$3{,}42E+11$	61 %

Regarding the braking manoeuvre studied here, the overall damage is almost only induced by the RR loadings. Then, the comparison between the value of reference D_{RFC} and the one based on the signal partition, using the same life assessment method $D_{R_{RFC}} + D_{D_{RFC}}$, gives quite a good match (only 6% gap). This result validates the overall partition method for this manoeuvre. Finally, especially for the Rayleigh approximation, the results between the use of the spectral methods and the reference value are close (only 4% gap). The method based on the Single Moment approximation still gives the same amount of inaccuracy as in Table 2, as expected.

5. Conclusion

This paper depicts the overall partition procedure performed on time-series to split the Driven Road loadings from the Random Road ones. The initial time-series comes from proving ground measures dealing with the usual 6 DOF per wheel and 12 DOF per axle on a vehicle. Inside the chassis system components, the loading measured is supposed multiaxial. The aim of this paper is to assess directly the partition process validity. Thus, some hypotheses are made regarding the stress tensor shape perceived at some relevant points of interest (i.e. linearity and unique stress orientation).

Driven Road loadings, as they are time-correlated, gives the opportunity to define "Driven" coefficients between the loads. Hence, a master signal can be defined to perform one and only one time the Rainflow counting method to define a master loading spectrum. Then, knowing the coefficients, the other Driven Road loadings spectra ensue from the master one. Regarding Random Road loadings, the stress orientation hypothesis provides the opportunity to perform the spectral methods directly on the signal measured at the wheel. These methods, when relevant, enable to assess the fatigue behaviour based on the signal power spectral density instead of the overall time-series.

The method is illustrated on real time-series while the vehicle performs a simple braking manoeuvre. For both methods, the damage calculation is performed using a Basquin equation with arbitrary parameters, not related to any material. Driven Road loadings are in this case F_X, F_Z and M_Y measured at the wheel. The master signal chosen is the longitudinal acceleration γ_x. To illustrate the method application, orientation coefficient are fixed to unity value. For each comparison, a reference damage is calculated based on the usual Rainflow counting method. The partition method leads to Random Road loadings that meet the requirements of the spectral methods. As a result, the application of the spectral methods on the one side, and the Rainflow counting method on the other side, gives quite good results regarding the life assessment indicator proposed.

Acknowledgements

This work was carried out within the framework of the partnership between Stellantis and the OpenLab Computational Mechanics with the financial support of the ANRT for the CIFRE contract n°2019/0764.

References

Grubisic, V., 1994, Determination of load spectra for design and testing, International Journal of Vehicle Design, Vol.15, pp. 8-26.

Sonsino, C. M., Heim, R., Melz, T., 2015, Why Variable Amplitude Loading? A Key for Lightweight-Structural Durability Design, in VAL3, 3rd International Conference on Material and Component Performance under Variable Amplitude Loading, pp. 73-80.

Matsuishi, M., & Endo, T., 1968, Fatigue of metals subjected to varying stresses, Paper presented to the Japan Society of Mechanical Engineers, Fukuoka, Japan.

Richlik, I., 1987, A new definition of the rainflow cycle counting method, International Journal of Fatigue, Vol.9, pp. 119-121.

Decker, M., 2020, Vibration fatigue-Lifetime of systems subject to shocks and vibrations, in VAL4, Proceedings of the 4th International Conference on Material and Component Performance under Variable Amplitude Loading, pp. 3-18.

Basquin, O. H., 1919, The exponential law of endurance tests, Proceedings of the ASTM, Vol.10, pp. 625-630.

Palmgren, A. G., 1924, Die Lebensdauer von Kugellagern - The Fatigue Life of Ball-Bearings (In German), Zeitschrift des vereins Deutscher Ingenieure, Vol.68, pp. 339-341.

Miner, M. A., 1945, Cumulative damage in fatigue, Journal of Applied Mechanics, Vol.12, pp. A159-A164.

Preumont, A., 1994, Random vibration and Spectral Analysis., Springer Netherlands.

Pitoiset, X., 2001, Méthodes spectrales pour une analyse en fatigue des structures métalliques sous chargements aléatoires multiaxiaux (in French), Doctoral dissertation, Université Libre de Bruxelles.

Rognon, H., 2013, Comportement en fatigue sous environnement vibratoire : prise en compte de la plasticité au sein des méthodes spectrales (in French), Doctoral dissertation, Ecole Centrale Paris.

Mršnik, M., Slavič, J., & Boltežar, M., 2013, Frequency-domain methods for a vibration-fatigue-life estimation – Application to real data, International Journal of Fatigue, Vol.47, pp. 8-17.

Rice, S., O., 1945, Mathematical analysis of random noise, Bell system technical journal, Vol.23, pp. 282-332.

Cartwright, D., & Longuet-Higgins, M., 1956, The statistical distribution of the maxima of a random function, Proceedings of Royal Society of London, Vol.237, pp. 212-232.

Miles, J., 1954, On structural fatigue under random loading, Journal of Aeronautical Sciences., Vol.21, pp. 753-762.

Benasciutti, D., Tovo, R., 2004, Rainflow cycle distribution and fatigue damage in Gaussian random loadings, report del dipartimento di ingegneria n°129, Università degli Studi di Ferrara.

Larsen, C., Lutes, L., 1990, Improved spectral method for variable amplitude fatigue prediction, Journal of Structural Engineering, Vol.116, pp. 1149-1164.